Aberrant High-Order Dependencies in Schizophrenia Resting-State Functional MRI Networks

Qiang Li[1*], **Vince D. Calhoun**[1], **Adithya Ram Ballem**[1], **Armin Iraji**[1,2*]
[1]Tri-Institutional Center for Translational Research in Neuroimaging and Data Science (TReNDS)
Georgia State University, Georgia Institute of Technology, Emory University, Atlanta, GA, USA
[2]Department of Computer Science, Georgia State University, Atlanta, GA, USA

Shujian Yu[3]
[3]Department of Computer Science
Vrije Universiteit Amsterdam, The Netherlands

Jesus Malo[4]
[4]Image Processing Laboratory
University of Valencia, Spain

Abstract

The human brain has a complex, intricate functional architecture. While many studies primarily emphasize pairwise interactions, delving into high-order associations is crucial for a comprehensive understanding of how functional brain networks intricately interact beyond simple pairwise connections. Analyzing high-order statistics allows us to explore the nuanced and complex relationships across the brain, unraveling the heterogeneity and uncovering patterns of multilevel overlap on the psychosis continuum. Here, we employed high-order independent component analysis (ICA) plus multivariate information-theoretical metrics (O-information and S-information) to estimate high-order interaction to examine schizophrenia using resting-state fMRI. The results show that multiple brain regions networks may be altered in schizophrenia, such as temporal, subcortical, and higher-cognitive brain regions, and meanwhile, it also shows that revealed synergy gives more information than redundancy in diagnosing schizophrenia. All in all, we showed that high-order dependencies were altered in schizophrenia. Identification of these aberrant patterns will give us a new window to diagnose schizophrenia.

1 Introduction

Schizophrenia is a major psychotic disease that severely affects people's quality of life, and it is usually characterized by delusions, hallucinations, disorganization, and unusual behavior. The pathogenesis behind schizophrenia is complex, multifaceted, and involves multiple brain regions, and previous studies have shown that pair-wise functional connectomics is altered as one of the features of schizophrenia [1–4]. However, pair-wise functional connectomics will not capture multiple network statistical relationships and will ignore some high-order functional interactions that may play an important role in its use as a biomarker for schizophrenia [5–7]. The related studies have shown that multivariate mutual information can be used as a high-order functional connectivity descriptor and applied to the diagnosis of psychotic disorders [8–14]. Therefore, in this study, we hypothesize that aberrant high-order dependencies are present in schizophrenia, and we investigate this using high model-order independent component analysis (ICA) plus information-theoretical metrics (O-information and S-information) to estimate high-order brain network interaction to examine schizophrenia using resting-state fMRI (rsfMRI).

Information-Theoretic Principles in Cognitive Systems Workshop at the 37th Conference on Neural Information Processing Systems (NeurIPS 2023).

2 Materials and Methods

2.1 rsfMRI Dataset

The total dataset of 1004 subjects from the Bipolar and Schizophrenia Network for Intermediate Phenotypes (BSNIP) consortium [15] (including 502 subjects in typical controls and 502 subjects diagnosed with schizophrenia) used in this work was obtained by using 105 intrinsic connectivity network (ICN) (see **Appendices**, in Fig. 3) time courses derived from a multi-spatial-scale, spatially constrained ICA approach, and this allows generalizability and comparability of findings across studies. The shape of the time course is [T, 105], where T is the number of time points that are different between subjects [16]. The rsfMRI preprocessed steps as shown in Fig. 1: (a.) Quality control was applied to identify high-quality data. (b.) Each subject's rsfMRI data were preprocessed using a common procedure, including rigid body motion correction, slice timing correction, and distortion correction. (c.) Preprocessed subject data were registered into a common space, resampled to $3mm^3$ isotropic voxels, and spatially smoothed using a Gaussian kernel with a $6mm$ full width at half-maximum. (d.) We used a multi-spatial-scale template of 105 ICNs obtained from 100k+ subjects and a constraint ICA approach to obtain subject-specific ICN time courses, and they were cleaned using a common standard. (e.) The estimated 105 intrinsic connectivity networks are categorized into visual (VI), cerebellar (CB), temporal (TP), subcortical (SC), somatomotor (SM), and higher cognitive (HC) groups for the next information theory analysis.

2.2 Information-Theoretical Analysis

The *Total Correlation (TC)* and *Dual Total Correlation (DTC)* describe the dependence among n variables and can be considered as a non-negative generalization of the concept of mutual information from two parties to n parties. Let the definition of total correlation due Watanabe [17] be denoted as:

$$\mathbf{TC}\left(X^1, \cdots, X^n\right) = \sum_{i=1}^{n} \mathbf{H}\left(X^i\right) - \mathbf{H}\left(X^1, \cdots, X^n\right) \tag{1}$$

where $\mathbf{H}(X^i)$ denotes marginal entropy, and $\mathbf{H}(X^1, \cdots, X^n)$ represents joint entropy. Analogously with *TC*, *DTC* can be defined as [18],

$$\begin{aligned} \mathbf{DTC}\left(X^1, \cdots, X^n\right) &= \mathbf{H}\left(X^1, \cdots, X^n\right) - \sum_{i=1}^{n} \mathbf{H}\left(X^i \mid X^{[n]\setminus i}\right) \\ &= \left[\sum_{i=1}^{n} \mathbf{H}\left(X^{[n]\setminus i}\right)\right] - (n-1)\mathbf{H}\left(X^1, X^2, \cdots, X^n\right) \end{aligned} \tag{2}$$

where $X^{[n]\setminus i} = \{X^1, \cdots, X^{i-1}, X^{i+1}, \cdots, X^n\}$, i.e., the set of all variables excluding X^i. From these definitions in Eqs. 1, 2, if all variables are independent, both *TC* and *DTC* will be zero.

From the *TC* and *DTC*, we get O-Information and S-Information, which capture the overall balance between redundant and synergistic high-order dependencies in multivariate system [19].

The O-Information of a set of n random variables X^n can be get as,

$$\mathbf{\Omega_n}\left(X^1, \cdots, X^n\right) = \mathbf{TC}\left(X^1, \cdots, X^n\right) - \mathbf{DTC}\left(X^1, \cdots, X^n\right) \tag{3}$$

The S-Information of a set of n random variables can be calculate as,

$$\mathbf{\Sigma_n}\left(X^1, \cdots, X^n\right) = \mathbf{TC}\left(X^1, \cdots, X^n\right) + \mathbf{DTC}\left(X^1, \cdots, X^n\right) \tag{4}$$

if *TC* $>$ *DTC* or $\mathbf{\Omega} > 0$, the system corresponds to redundancy-dominated dependencies, and in the other way around, *DTC* $>$ *TC* or $\mathbf{\Omega} < 0$, the system corresponds to synergy-dominated dependencies [19].

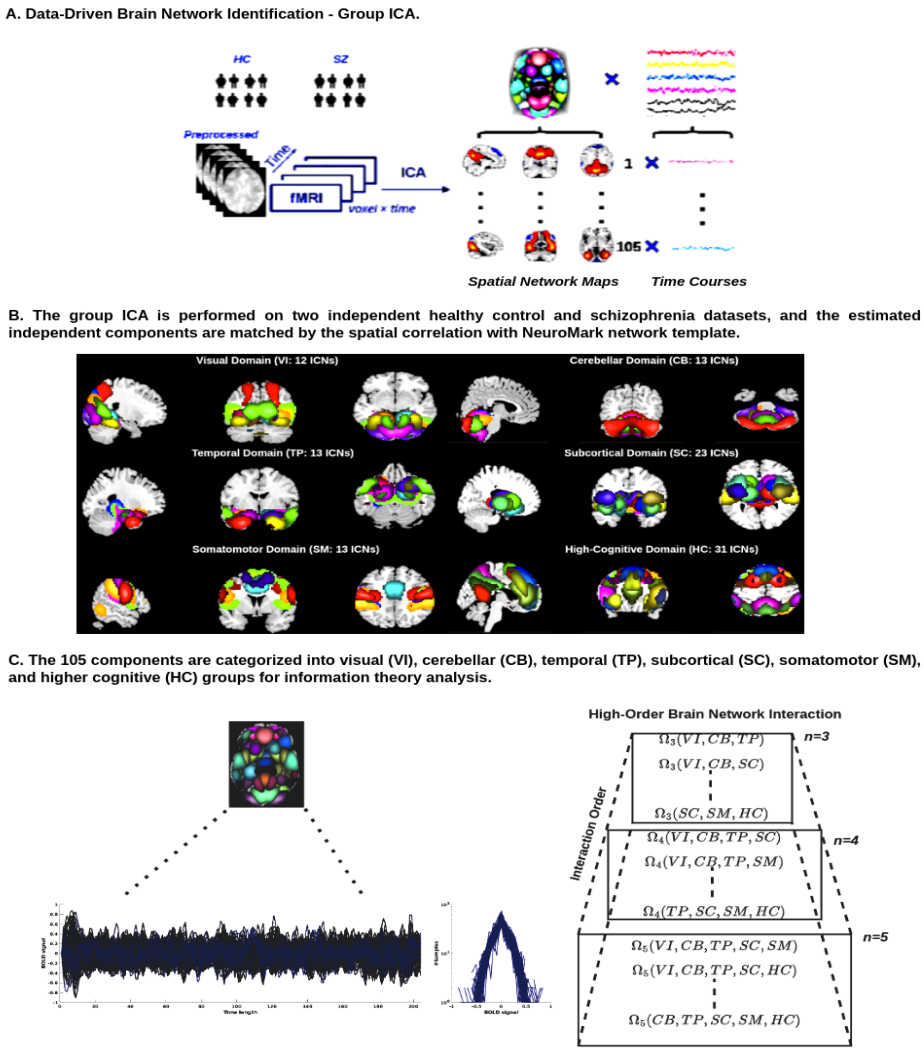

Figure 1: Flowchart of capturing high-order dependencies among brain connectivity states. **A.** Group ICA is performed on two independent healthy control and schizophrenia datasets, and corresponding 105 spatial network maps and time courses are extracted from each subject. **B.** The estimated independent components are matched with the NeuroMark_2.1 template [16] based on spatial correlation, and then all components are categorized into six groups, i.e., VI, CB, TP, SC, SM, and HC. **C.** The BOLD signal from independent components matches a multivariate Gaussian distribution and related high-order (i.e., interaction order: 3, 4, 5) information measures with O-information and S-information.

Consider the fMRI signal as a Gaussian distribution, as shown in Fig. 1C, and for a univariate Gaussian random variable $X \sim \mathcal{N}(\mu, \sigma)$, the entropy (given in nats) will be $\mathbf{H}^{\mathcal{N}}(X) = \frac{\ln\left(2\pi e \sigma^2\right)}{2}$, and for a multivariate Gaussian distribution, the joint entropy will be $\mathbf{H}^{\mathcal{N}}\left(\left(X^1, \cdots, X^n\right)\right. = \frac{\ln[(2\pi e)^n |\Sigma|]}{2}$, where $|\Sigma|$ refers to the determinant of the covariance matrix of $\left(X^1, \cdots, X^n\right)$. For the multivariate Gaussian case, the mutual information between $\left(X^1, \cdots, X^n\right)$ and $\left(Y^1, \cdots, Y^n\right)$ is given by, $\mathbf{I}((X^1, \cdots, X^n); (Y^1, \cdots, Y^n)) = \frac{1}{2\ln 2} \ln\left[\frac{\left|\Sigma_(X^1, \cdots, X^n)\right|\left|\Sigma_(Y^1, \cdots, Y^n)\right|}{\left|\Sigma_{(X^1, \cdots, X^n)(Y^1, \cdots, Y^n)}\right|}\right]$. Finally, the Gaussian estimator for total correlation can be:

$$\mathbf{TC}^{\mathcal{N}}\left(X^1, \cdots, X^n\right) = \frac{-\ln(|\Sigma|)}{2} \tag{5}$$

From [20], the Eq. 3, 4 will be changed to,

$$\mathbf{\Omega_n}^{\mathcal{N}}\left(X^1,\cdots,X^n\right)=(2-n)\mathbf{TC}^{\mathcal{N}}\left(X^1,\cdots,X^n\right)+\sum_{i=1}^{n}\mathbf{TC}^{\mathcal{N}}\left(X^{[n]\setminus i}\right) \tag{6}$$

By referencing Eqs. 3, 4, 5, and 6, all the metrics described above can be computed, i.e., *TC*, *DTC*, *O*-information and *S*-information for multivariate Gaussian variables.

3 Results and Discussion

The low-order functional connectivity (LOFC), based on pairwise Pearson correlation in healthy control subjects(HCS) and schizophrenia patients (SCS), is illustrated in Fig.2 and Fig.4 (see **Appendices**). We see that major aberrant brain network interaction happened between visual-somatomotor and temporal-high cognitive brain areas, and it reflects that three brain networks, such as visual, somatomotor, and higher cognitive, may be altered in the SCS.

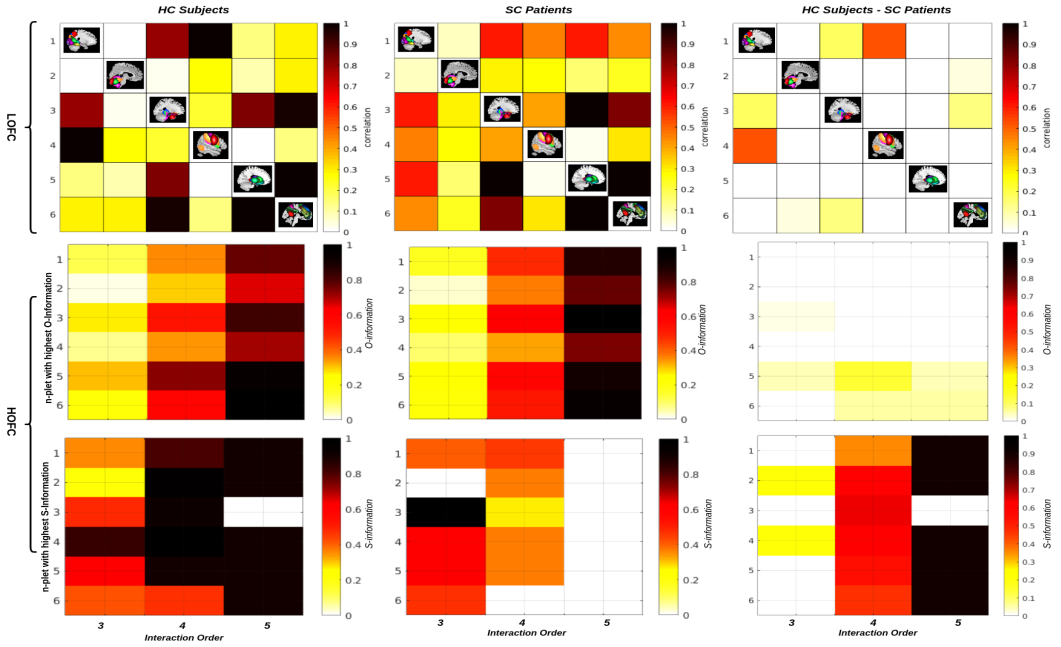

Figure 2: Comparison of low-order functional connectivity (LOFC) and high-order functional connectivity (HOFC) between HCS and SCS . The top row shows that LOFC and the main difference present a pair-wise interaction between VI-SM and TP-HC. The bottom row presents the HOFC with redundancy and synergy information-theoretic measures made from HCS and SCS, and the HOFC not only captures redundancy information but also synergy information in the human brain, and with interaction order increasing, we see that more difference is captured by the HOFC.

In high-order functional connectivity (HOFC), both the integration and segregation of brain information networks are depicted using multivariate information theory measures (in Fig. 2). The analysis reveals that redundancy information is predominantly distributed across the brain regions of both SCS and HCS, with interaction order gradually increasing. Notably, it captures more aberrant brain networks, including TP, SC, and HC brain regions. This observation may imply the involvement of these brain regions in schizophrenia patients. Moreover, synergy information was also uncovered by HOFC, and it showed that synergy information plays a more important role than redundancy in SCS, and it may suggest that synergy is mainly aberrant in SCS, as it can be a biomarker for diagnosing SCS.

However, there are still some limitations, and the next step would be to dig into specific independent component networks and see which independent component networks mainly contribute to the SCS.

Second, explaining the role of redundancy and synergy in the SCS and how to properly explain them from a neurophysics perspective.

References

1. Fu, Z. *et al.* Dynamic state with covarying brain activity-connectivity: On the pathophysiology of schizophrenia. *NeuroImage* **224,** 117385 (2021).
2. Meng, X. *et al.* Multi-model order spatially constrained ICA reveals highly replicable group differences and consistent predictive results from resting data: A large N fMRI schizophrenia study. *NeuroImage: Clinical* **38,** 103434 (2023).
3. Du, Y. *et al.* Evidence of shared and distinct functional and structural brain signatures in schizophrenia and autism spectrum disorder. *Communications Biology* **4** (Sept. 2021).
4. Iraji, A. *et al.* Spatial Dynamic Subspaces Encode Sex-Specific Schizophrenia Disruptions in Transient Network Overlap and its Links to Genetic Risk. *bioRxiv : the preprint server for biology* (July 2023).
5. Xie, Q. *et al.* Constructing high-order functional connectivity network based on central moment features for diagnosis of autism spectrum disorder. *PeerJ* **9,** e11692 (2021).
6. Zhang, Y., Zhang, H., Chen, X., Lee, S.-W. & Shen, D. Hybrid high-order functional connectivity networks using resting-state functional MRI for mild cognitive impairment diagnosis. *Scientific reports* **7,** 6530 (2017).
7. Chen, X. *et al.* High-order resting-state functional connectivity network for MCI classification. *Human brain mapping* **37,** 3282–3296 (2016).
8. Herzog, R. *et al.* Genuine high-order interactions in brain networks and neurodegeneration. *Neurobiology of Disease* **175,** 105918 (2022).
9. Li, Q. *Measuring Functional Connectivity of Human Intra-Cortex Regions with Total Correlation* in *Entropy 2021: The Scientific Tool of the 21st Century* (May 2021), 9797.
10. Li, Q. Functional connectivity inference from fMRI data using multivariate information measures. *Neural Networks* **146,** 85–97 (2022).
11. Li, Q., Steeg, G. V., Yu, S. & Malo, J. Functional Connectome of the Human Brain with Total Correlation. *Entropy* **24,** 1725 (2022).
12. Li, Q., Steeg, G. V. & Malo, J. Functional connectivity in visual areas from Total Correlation. *arXiv preprint arXiv:2208.05770* (2022).
13. Li, Q., Yu, S., Madsen, K. H., Calhoun, V. D. & Iraji, A. *Higher-Order Organization in the Human Brain From Matrix-Based Rényi's Entropy* in *2023 IEEE International Conference on Acoustics, Speech, and Signal Processing Workshops (ICASSPW)* (2023), 1–5.
14. Gatica, M. *et al.* High-order interdependencies in the aging brain. *Brain connectivity* **11,** 734–744 (2021).
15. Tamminga, C. A. *et al.* Clinical phenotypes of psychosis in the Bipolar-Schizophrenia Network on Intermediate Phenotypes (B-SNIP). *American Journal of psychiatry* **170,** 1263–1274 (2013).
16. Iraji, A. *et al.* Canonical and Replicable Multi-Scale Intrinsic Connectivity Networks in 100k+ Resting-State fMRI Datasets. *bioRxiv* (Sept. 2022).
17. Watanabe, S. Information theoretical analysis of multivariate correlation. *IBM Journal of research and development* **4,** 66–82 (1960).
18. Han, T. S. Nonnegative Entropy Measures of Multivariate Symmetric Correlations. *Inf. Control.* **36,** 133–156 (1978).
19. Rosas, F. E., Mediano, P. A., Gastpar, M. & Jensen, H. J. Quantifying high-order interdependencies via multivariate extensions of the mutual information. *Physical Review E* **100,** 032305 (2019).
20. Varley, T. F., Pope, M., Faskowitz, J. & Sporns, O. Multivariate information theory uncovers synergistic subsystems of the human cerebral cortex. *Communications Biology* **6** (2022).
21. Coifman, R. & Lafon, S. Diffusion maps. *Applied and Computational Harmonic Analysis* **21,** 5–30 (July 2006).

4 Appendices

4.1 Independent Component Networks

Total of 105 independent component networks identified from multivariate spatially constrained ICA are shown in Fig. 3.

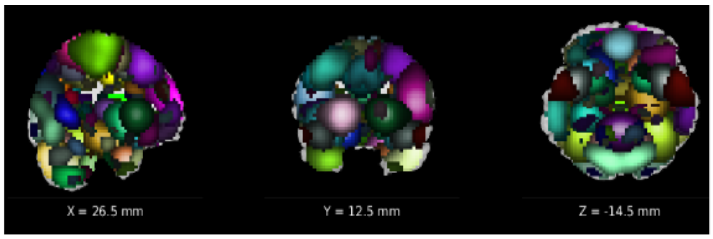

Figure 3: A total of 105 independent component networks are presented on the overlay brain volume, and different colors refer to each independent component network. Each component is also displayed separately.

4.2 Low-Order Functional Connectogram

The low-order functional connectivity estimated for 105 independent component networks, and we applied the diffusion embedding algorithm [21] to cluster the related independent component networks.

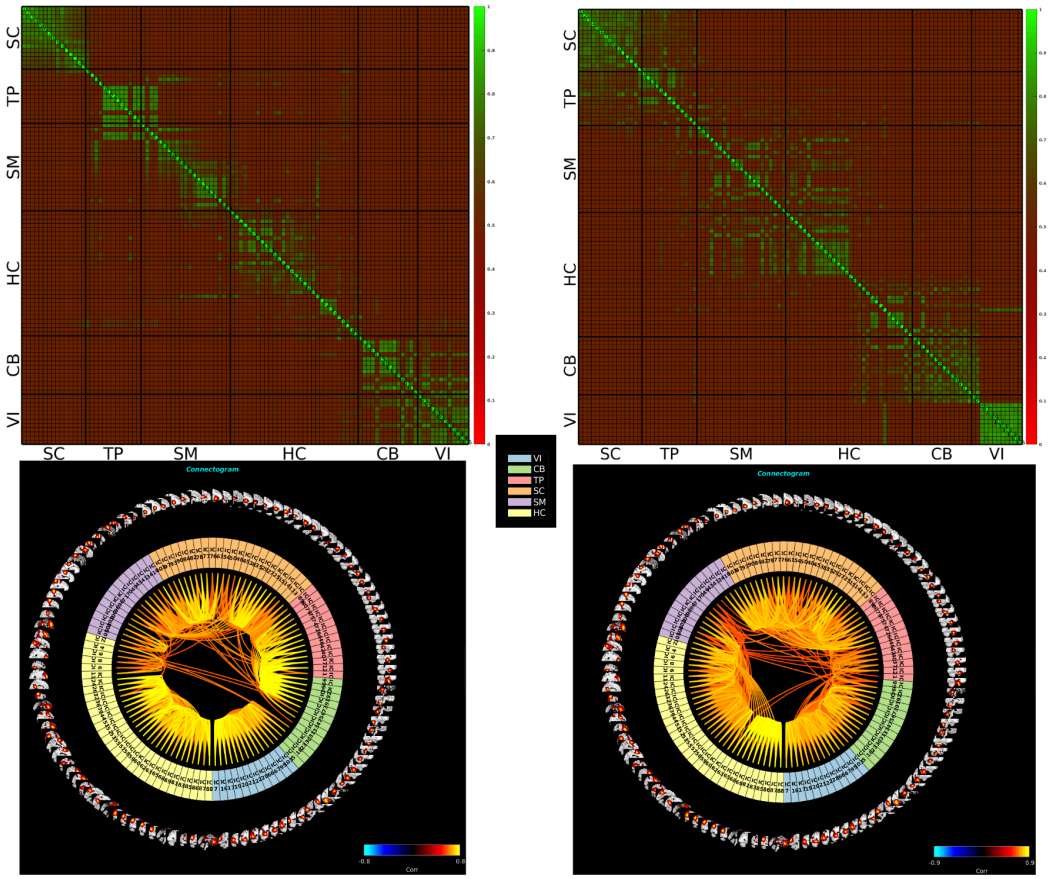

Figure 4: Comparison of clustering low-order functional connectivity (LOFC) between healthy controls (HCS, left side) and schizophrenia (SCS, right side) The top row shows that LOFC presents a pair-wise interaction. The bottom row presents the functional connectogram corresponding to each correlation map with a threshold set to 0.6.

Here we clearly see that interaction-independent component network patterns are clumped, and the pattern can be matched to six multi model order ICA brain template networks (see Fig. 4). The corresponding functional connectogram was also presented with a threshold of 0.6.

4.3 High-Order Functional Connectogram

Given the number of independent component networks, exploring the high-order functional connectogram with 105 independent component networks along with increasing interaction order will face some challenges. Furthermore, it will also face how to present the result with a graph connectogram, and all these problems will be major problems that need to be solved, but it will be very important for us to precision diagnose schizophrenia, and the previous related research [11] has already provided us with a window to solve it, and we can apply it to the precision diagnosis of schizophrenia.